Polymer Bulletin 30, 313–320 (1993)

Polymer Bulletin

Interpretation of ^{2}H-NMR lineshapes of PEO

D. Reichert* and H. Schneider

Technical University Merseburg, Department of Physics, O-4200 Merseburg, Germany

Summary

Temperature dependent ^{2}H-nmr lineshapes and relaxation times T_{2e} of poly(ethylene oxide) (PEO_d) and two block copolymers of deuterated PEO_d and protonated poly(butyl methacrylate) ($PBMA_h$) were measured. The results were compared with simulated lineshapes and relaxation times and discussed as the glass transition of PEO chains.

Introduction

One of the principal objects of polymer research is to investigate molecular dynamics in bulk polymeric systems. Besides a variety of other techniques, nmr methods are often used. Because it has certain advantages ^{2}H-solid state nmr plays an important role in these techniques. To ask about molecular dynamics often means to ask about (i) geometry and (ii) the time constant of a molecular motion. The term "geometry" means the geometrical position of sites which can be occupied by a jumping C-D bond; the time constant is then simply the reciprocal jump frequency. Using the ^{2}H-solid echo technique, it is possible to determine both geometry and time scale in a "time window" from 10^{-3} to 10^{-7}s (1), (2). For faster motions, only the geometry can be determined from lineshape studies; slower motions require the use of spin-alignment techniques (5). In a homogeneous probe, the treatment for evaluating molecular dynamics is in principle straightforward: make an approximation of the molecular geometry (e.g. methylrotation, phenyl flip, gauche-trans isomerization), calculate corresponding lineshapes for different jump frequencies and compare these with experimental results. To get an ARRHENIUS plot (log(Ω) vs. T), these procedure must be done for different temperatures.

However, some differences occur when deuterons are placed in heterogeneous media. For example, let's look at a semicrystalline polymer above the glass transition temperature T_g but below the melting point T_m: in this case the deuterons in the amorphous phase are highly movable (i.e. they are jumping with a high frequency), whereas those in the crystalline phase are rigid in the nmr-time scale (they are jumping with a lower frequency). Consequently, the experimental lineshape is the superposition of a "high-frequency lineshape" (for example a single line at $\omega = \omega_o$) and a "low frequency lineshape" (for example a PAKE pattern) (6).

To determine whether an observed lineshape comes from a deuteron in a homogeneous medium (all deuterons are jumping with the same frequency) or from deuterons in different phases with different mobilities, one needs additional experimental values: relaxation times T_1 and T_{2e} (2), (9). Depending on the class of lineshape explained above, a single T_1 (in a homogenous system) or a multicomponent T_1 (in heterogenous systems) occur. In protonated

*Corresponding author

heterogeneous systems the multicomponent T_1 is often masked by spin diffusion effects (3). However, because of the low level of dipolar coupling, spin diffusion can be neglected for deuterated systems. The relaxation time T_{2e} depends on the jump frequency Ω. The T_{2e} vs. T representation exhibits one minimum at the temperature when $\Omega \approx \omega_Q$ for a homogeneous probe or two or more minima (one minimum for each process which reached the temperature where the condition $\Omega_i(T) \approx \omega_Q$ is fulfilled) or a more complicated behavior for heterogeneous probes.

The aim of this paper is to present ^{2}H-nmr lineshapes and T_{2e} measurements on poly(ethylene oxide) (PEO) and on a block-copolymer of PEO and poly(butyl methacrylate) (PBMA).

Experimental

All experiments were performed using the homebuilt spectrometer HFS 270 (University of Leipzig, Department of Physics) operating at 41.5 MHz for ^{2}H. Line-shape measurements were performed using the solid-echo pulse sequence $(\pi/2)_{0°}$-τ-$(\pi/2)_{90°}$-echo (7). Because of the capabilities of the spectrometer equipment, all time domain signals were recorded in the single detection mode. Consequently, in the frequency domain only half of the (symmetrical) spectrum appears starting from ω_0. To allow easy comparison of the experimental spectrum with simulated lineshapes (which exhibit both frequency directions around ω_0), the former were expanded to quadratur-detection spectra by zero filling prior to FOURIER transformation. Because of the strong symmetry of the quadrupolar interaction relative to the sign of ω_Q, no information loss or artifacts occur when using this procedure.

For easy comparison of the experimental spectrum $I_{exp}(\omega)$ with the simulated lineshape $I_{sim}(\omega)$, it is necessary also to include a frequencydependent spectral correction for finite pulse length. This correction $C(\omega)$ is known as the "BLOOM-correction" (8) and it includes simultaneous action of the pulse- and quadrupolar Hamiltonian during pulses. The correction can be done by dividing the experimental spectrum by the correction $(I_{exp}(\omega)/C(\omega) \Longleftrightarrow I_{sim}(\omega))$ or by multiplying the simulated lineshape with the correction $(I_{exp}(\omega) \Longleftrightarrow I_{sim}(\omega) \bullet C(\omega))$. We used the latter procedure because the noise in the wings of the spectrum is increased dramatically using the former ($C(\omega)$ goes to zero for large $\Delta\omega = \omega_0 - \omega$). Typical achievable pulse length of 8 μs for $\pi/2$ pulses leads to a substantial distortion of lineshapes (for example, the typical PAKE pattern at low temperatures is strongly falsified; see fig. 2). However, the mean features of the lineshapes are visible; a reliable evaluation is possible still nevertheless.

To determine the relaxation time T_1, it is unacceptable to use the common inversion-recovery sequence because of the substantial spectral distortions due to finite pulse length. This is why we used a saturation sequence consisting of solid-echo experiments repeated with different repetition times t_{rep} with $(\pi/2)_{0°}$-τ-$(\pi/2)_{90°}$-τ-echo-t_{rep} ($\tau \ll t_{rep}$). T_1 is then determined by fitting the echo amplitude $S(t_{rep})$ depending on t_{rep} to a mono- or multiexponential decay with time constant T_1.

The relaxation time T_{2e} is defined as the decay time of the solid-echo amplitude $SE(\tau)$ depending on the pulse delay time τ. Note that the amplitude of the solid echo (i.e. the magnetization) for a constant $\tau > 0$ (used in (2)) exhibits with respect to Ω the same features T_{2e} with respect to Ω, particularly the minimum for $\Omega \approx \omega_Q$, and thus it contains the same information. Ω depends on T via ARRHENIUS or WLF (14). However, the signal amplitude $SE(\tau)$ vs. T is influenced also by the repetition time t_{rep} (T_1-effect) and by the temperature dependence of the magnetization (CURIE's law). The valve T_{2e} is free of these influences.

Unfortunately the decay of SE(τ) is often nonexponential (also in a homogeneous system (9)) and thus it is difficult to determine a decay time. We used a T_{2e} defined by the decay of SE(τ) from τ=50μs to τ=100μs

$$T_{2e} = \frac{50\mu s}{\ln\left(\frac{SE(50\mu s)}{SE(100\mu s)}\right)} \quad (1)$$

Table 1: Characterization of used sample (α: degree of crystallinity)

	PEO	PEO/PBMA 1:5		PEO/PBMA 5:1	
		PEO	PBMA	PEO	PBMA
M_n/g:mol	9600	8000	40000	36800	7700
α /%	78	?	-	49	-
T_m^{PEO}/K	334	319	-	322	-
T_g^{PBMA}/K	-	-	?	-	350

As a sample we used PEO_d and two block-copolymers of PEO_d-$PBMA_h$ prepared by anionic polymerization (10). Table 1 summarizes some characteristics of the samples. M_n was determined from the amount of monomers prior polymerization. It agrees with experimental values within experimental error. melting temperature T_m(PEO), glass transition temperature T_g(PBMA) and degree of crystallinity α were determined by DSC (11). Because of the equipment, it was not possible to determine T_g(PEO) (11). All samples were sealed in nmr tubes without any thermal treatment after polymerization. Experiments were performed in a temperature range from 140 K to 290 K.

Line-shape simulation

To calculate lineshapes $I_{sim}(\omega)$ of jumping C-D bonds between N unequivalent sites dependent on Ω we used the treatment of WITTEBORT (2). To specify the jump geometry it is advantageous to introduce a molecular frame with the Z-axis parallel to the symmetry axis of the jump motion. The jump geometry is then easy to describe by a set of polar- and azimuth angles β_i and ϕ_i specifying the N different orientations of the observed C-D bond in this frame. In our case the labeled polymer (PEO) contains deuterons in the backbone only. Consequently, we used as a model for this main chain motion a 3-fold jump (gauche-trans isomerization). For β_i and ϕ_i we assume that

$$\beta_i = 54.7°$$

$$\phi_1 = 0°,120°,240° \qquad (2)$$

$$i = 1,2,3 .$$

It is well known (13) that because of the helical structure of PEO the population of the symmetrically occupied gauche configurations are preferred respective to the trans configuration. Therefore, an additional parameter p_t (trans population) is introduced and each gauche population p_g is consequently

$$p_g = \frac{1}{2}(1 - p_t) . \qquad (3)$$

Fig. 1 shows simulated lineshapes for different jump frequencies Ω and equally populated sites. The most characteristic feature is the change from a PAKE pattern for slow motion over an apparent superposition of PAKE pattern and a single line to a single line for fast motion.

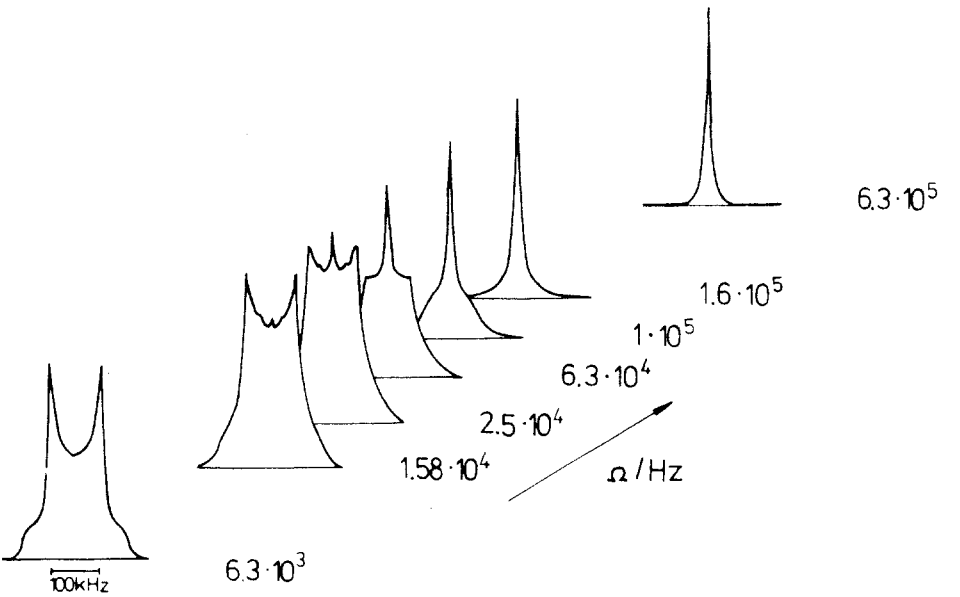

Fig.1: Simulated lineshapes for gauche-trans isomerization (eq. 1) and equal populated sites

Because of the amorphous nature of polymers one often finds distributions DF(Ω) of jump frequencies Ω (14), (15). It was also necessary for our investigations to include a log-GAUSSIAN distribution (LGD) to explain experimental results. To do this we calculated lineshapes $I_{sim}(\omega,\Omega_i)$ for different Ω_i in steps of 0.1 Ω_i decades and superposed these

lineshapes according to

$$I(\omega,\Omega_0,\delta) = \sum_i DF_{LGD}(\Omega_i,\Omega_0,\delta)\cdot I(\omega,\Omega_i) \; . \tag{4}$$

The distribution function DF_{LGD} of a LGD is

$$DF_{LGD}(\Omega,\Omega_0,\delta) = \delta^{-1}\cdot(2\pi)^{-1} \cdot \exp\left(-\frac{\ln^2(\Omega/\Omega_0)}{2\delta^2}\right) . \tag{5}$$

Ω_0 is the mean frequency, δ the width of the distribution. Besides LGD, other distribution functions such as FOUSS-KIRKWOOD or COLE-COLE are often used (14). However, the best fit of our experimental values was achieved using a LGD. Note that a distribution of Ω influences not only the lineshapes but also broadens the T_{2e} minima with respect to Ω.

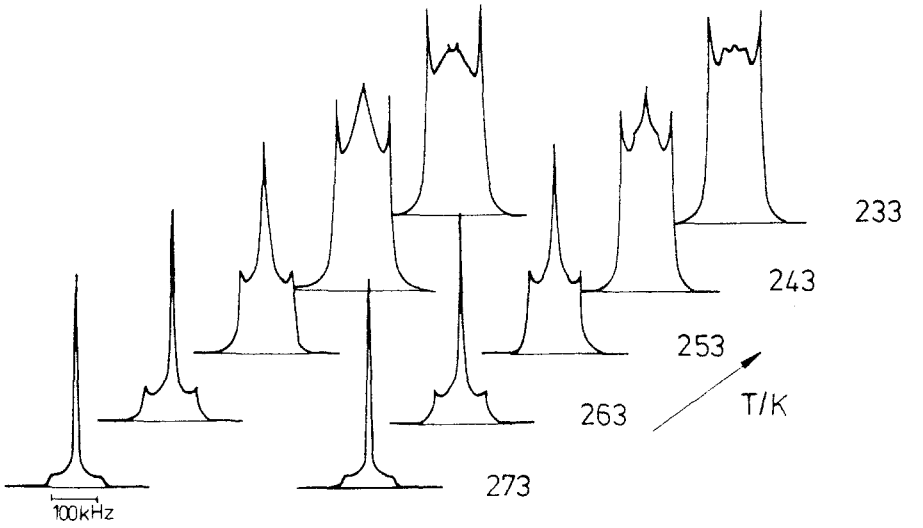

Fig.2: Temperature dependence of lineshapes (full symbols: experimental data, open symbols: simulated data)
●:PEO ▲:PEO/PBMA 5:1 ▼:PEO/PBMA 1:5

Experimental results

The left-hand side of fig. 2 displays temperature dependent spectra $I_{exp}(\omega)$ of the sample PEO_d-$PBMA_h$ 5:1. The main feature is the change with temperature from a PAKE pattern for $T < 230$ K (masked by the spectral distortion due to finite pulse length; see chap. 2) to a single line for $T > 273$ K. Furthermore, the T_1-decay is monoexponential for all temperatures

and T_{2e} exhibits a minimum at T≈255 K (see fig. 3). The experimental spectra can be explained either by a superposition of a PAKE pattern and a single line with an temperature dependent portions (the amount of slowly jumping C-D-bonds decreases with temperature, whereas the portion of quickly jumping bonds increases) or by a homogeneous motional process like that defined by eq. (5) which yields the lineshapes in fig. 1. Both assumptions give rise to nearly the same lineshapes. However, using relaxation times to decide between the two ways of interpreting the experimental spectra it is clear that the first assumption contrasts with the monoexponential T_1-decay and must thus be canceled. Moreover, the assumption of a homogeneous motional process is supported by the experimental T_{2e} vs. T behavior: it exhibits a minimum at those temperatures where the changes in lineshapes are most significant (see fig. 3). Assuming a molecular process with a geometry defined in eq. (5) and a LGD of jump rates it is possible to simulate both lineshapes and the shape of T_{2e} dependent on temperature within the limits of experimental error (only the lineshapes were fitted to experimental data; "simulated T_{2e}" were calculated from the results of lineshape fitting using eq. 1). Unfortunately, the absolute values of simulated T_{2e} are larger than the experimental values by a factor of five. So far we have no explanation for this fact. However, because the temperature of the minimum and the shape of T_{2e} vs. T agrees well with experimental values, we used this as a confirmation of our assumption of a unique motional process (i.e., a homogeneous mo-

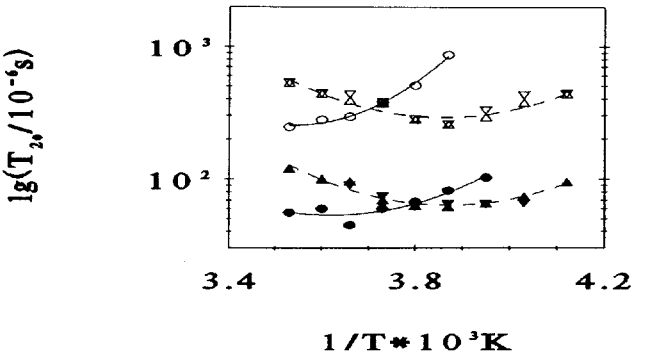

Fig.3: Temperature dependence of T_{2e} (full symbols: experimental-data, open symbols: simulated data)
●:PEO ▲:5:1 ▼:1:5

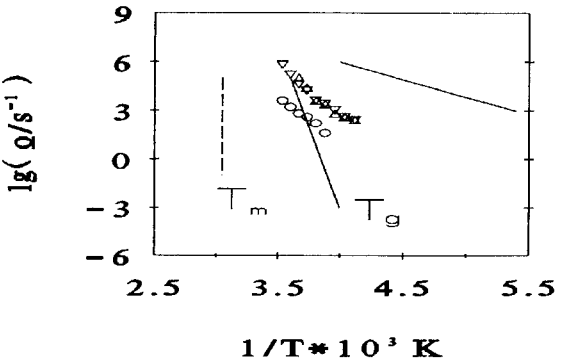

Fig.4: ARRHENIUS plot of PEO
○: PEO
△: PEO-PBMA 5:1
▽: PEO-PBMA 1:5

lecular dynamics).

Discussion

The final result of our investigation is the temperature dependence of the jump rates and the width of their distribution. These values are shown in figs. 4 and 5.

What conclusions can be drawn concerning the molecular dynamic of the polymer chains?

(i) It is clear from fig. 4 together with the motional model of a main-chain motion that the motional process of the PEO-main chains observed is the glass transition of PEO chains.

(ii) The temperature dependence of the glass transition of homo PEO (i.e. the curve Ω vs. 1/T; now abbreviated as "dynamic T_g") differs from that of the block copolymers, whereas the dynamic T_g of both block copolymers exhibits **no** difference in the error limit of our experiment (i.e., the dynamic T_g **does not** depend on the M_n of the polymer blocks in this case). Note that the $T_g(M_n)$ of PEO generally **does not** depend **monotonously** on M_n but exhibits a maximum at $M_n \approx 10^4$ g/mol (11). Obviously, this effect of M_n on T_g is completely masked by the influence of the microstructure on T_g. We explain this by the influence of the PBMA-chains: These chains in the vicinity of PEO domains decrease the "order" of the PEO-chains, and thus decrease the glass-transition temperature.

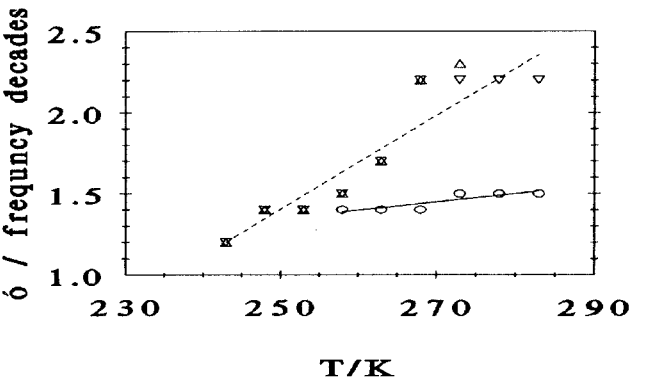

Fig.5: Width of LGD vs. temperature
○:PEO ▵:5:1 ▽:1:5

(iii) We **do not** observe separated T_g's for crystalline and amorphous PEO. We suppose that both amorphous and crystalline T_g's are masked by the broad distribution of Ω (see fig. 5).

(iv) Moreover, no interlayer (in the sense of a portion of PEO chains in which molecular dynamics are strongly influenced by PBMA chains) was detected (note that the result of our simulations was a **unique** dynamic process). However, because of the difference in molecular mobility of the PEO chain at T_g and PBMA chains well below T_g(PBMA) (see tab. 1) and because of the connection of the two blocks by a chemical bond such an interlayer must exist. We suppose that it is also masked by the distribution of Ω. Particularly the fact that the width of the LGD of Ω for the block copolymers increases

more then that for PEO (see fig. 5) points particularly to this explanation: the chains in the rest of the block move faster with increasing temperature, whereas those in the underlayer are attached to the "rigid" PBMA chain and cannot move as fast as the rest.

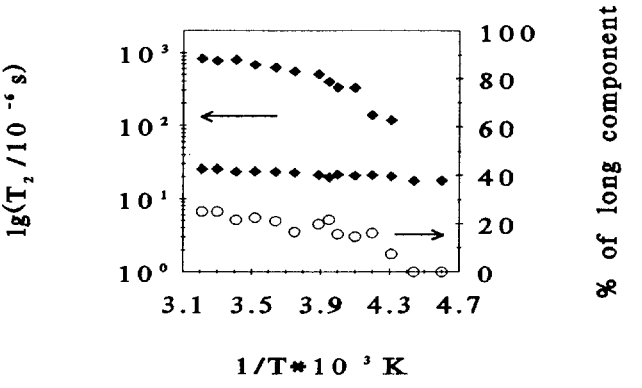

Fig.6: ^{1}H-T_2 vs. T for PEO/PBMA 5:1

Consequently, the width of the distribution of Ω broadens. However, in ^{1}H-T_2 experiments we find an interlayer: in a polymer well below T_g we expect for the relaxation time T_2 a constant value on the order of $T_2 \approx 10$ μs. This is true below T≈250 K for PEO-PBMA 1:5 and T≈235 K for PEO-PBMA 5:1. From this temperature a second component with a substantially increasing T_2 and a slightly increasing portion p_l appears (fig. 6). This points to an increased molecular mobility of a portion of the monomeric units in PBMA and thus to the interlayer. With the portions p_l from both samples and SAXS data (11) we get a thickness of the interlayer (in PBMA !) of ≈ 3..4 nm.

References

(1) H.W. Spiess, Chem. Phys. 6,217 (1974)
H.W. Spiess, H. Sillescu, J. Magn. Res. 42,381 (1981)
(2) R.J. Wittebort, E.T Olejniczak, R.G. Griffin, J. Chem. Phys 86,5411 (1987)
(3) A.D. Booth, K.J. Packer, Molec. Phys. 62,811 (1987)
W. Schenk, D. Reichert, H. Schneider, Polymer 71,329 (1990)
(4) H.W. Spiess, Coll. & Polym. Sci 261,193 (1983)
(5) H.W. Spiess, J. Chem. Phys. 72,6755 (1980)
(6) P.M. Heinrichs, J.M. Hevitt, M. Lindner, J. Magn. Res. 60,280 (1984)
(7) J.H. Davis, K.R. Jeffry, M. Bloom, M.I. Valic, Chem. Phys. Lett. 42,390 (1976)
(8) M. Bloom, J.H. Davis, M.I. Valic, Canad. J. Phys. 58,1510 (1980)
(9) D. Reichert, Phil. thesis, Merseburg 1990
(10) H. Reuter, Phil. thesis, Merseburg 1989
(11) R. Unger, Phil. thesis, Merseburg 1990
(12) B.T. Smith, J.M. Boyle, B.S. Garbow, Y. Ikobe, V.C. Klemm, C.B. Mole, "Matrix Eigensystem Routines-EISPACK Guide", Berlin (1974)
(13) J. Lange, Phil. thesis, Merseburg 1990
(14) V.D. Fetodov, H. Schneider, "NMR-Basic Principles & Progress", Springer Verlag Berlin, Heidelberg, New York 21 (1989)
(15) C. Schmidt, K.J. Kuhn, H.W. Spiess, Progr. Coll. & Polym. Sci. 71,71 (1985)

Accepted January 11, 1993 C